Available online at www.sciencedirect.com

ScienceDirect

Solar Energy 105 (2014) 656–668

SOLAR ENERGY

www.elsevier.com/locate/solener

Theoretical and experimental study on heat pipe cooled thermoelectric generators with water heating using concentrated solar thermal energy

Ashwin Date *, Abhijit Date, Chris Dixon, Aliakbar Akbarzadeh

RMIT University, School of Aerospace, Mechanical and Manufacturing Engineering, Bundoora East Campus, Melbourne, Australia

Received 26 December 2013; received in revised form 26 February 2014; accepted 16 April 2014
Available online 21 May 2014

Communicated by: Associate Editor Yanjun Dai

Abstract

This paper presents the theoretical analysis and experimental validation on the transient behaviour of a proposed combined solar water heating and thermoelectric power generation system. The proposed system consists of concentrated solar thermal device that provides a high heat flux source for thermoelectric generators. Thermoelectric generators are passively cooled using the heat pipes that are embedded inside a heat spreader block. The heat pipe condenser is immersed in a water tank. The immersed liquid cooling technique offers high heat transfer coefficient for cooling of the thermoelectric generators as well as a way to scavenge the heat through water heating that can be used for domestic or industrial purpose. Theoretical analysis develops the governing equations for the proposed system. Results from a scaled down lab setup are used to validate the theoretical analysis. For a flux of 50,000 W/m^2 a temperature difference of 75 °C across the thermoelectric generator can be achieved and the hot water can be heated up to 80 °C which can be used for domestic or industrial applications. With 75 °C temperature difference across the TEG hot and cold side, an open circuit voltage of 3.02 V can be generated for each thermoelectric generator with dimensions of 40 mm × 40 mm.

Keywords: Thermoelectric generators; Passive cooling; Heat pipes; Water heating

1. Introduction and background

Solar water heating systems are a mature technology that is well established and being widely used in many countries. The very first hot water system was introduced in the United States in 1871 by Clarence M. Kemp (Butti and Perlin, 1981). During the early 1900s many researchers focused on research related to solar water heating. Around 1909 a thermosyphon was used for the first time in solar water heating systems (Butti and Perlin, 1979). Until 1930 most of the domestic water heating was supported by coal fired boilers (Kalogirou, 2009). Solar water heating systems became real commercial products towards the 1960s (Best and Riffat, 1995). The 1973 oil crisis gave a major initiative to boost research in the field of solar water heating systems in the United States (Best and Riffat, 1995).

Solar water heating systems are becoming more well-known and now contribute significantly to global energy capacity (Global status report, 2013). China currently dominates the solar thermal market globally, in terms of total global share and also in terms of the annual growth in the global share of solar water heating. Apart from China, countries like Germany, Turkey, Brazil and India

* Corresponding author.
E-mail address: ashwin.date@student.rmit.edu.au (A. Date).

http://dx.doi.org/10.1016/j.solener.2014.04.016
0038-092X/

Nomenclature

q''_{in}	solar radiation flux incident of Fresnel lens (W/m^2)
$\dot{q}_h$	concentrated solar radiation on the target (W)
$\dot{q}_l$	heat loss rate from the water storage tank (W)
$\dot{q}_{l-tar}$	heat loss rate from the target of solar concentration (W)
$\dot{W}_{TEG}$	power generated by thermoelectric generator (W)
A_{lens}	aperture area of the lens (m^2)
$A_{hp-cond}$	outer surface area of condenser section of a heat pipe (m^2)
η_{lens}	optical efficiency of lens
t	time (s)
$q''_{w_{hp}}$	heat flux at the inter face of heat pipe and water in tank (W/m^2)
$\dot{q}_w$	heat input to the hot water in the storage tank (W)
$\dot{q}_l$	heat lost from the hot water storage tank (W)
m	mass of water in the storage tank (kg)
c_p	specific heat of water (kJ/kg K)
T_w	temperature of water in the tank (°C)
T_a	ambient temperature (°C)
T_i	initial temperature of water in the tank (°C)
T_c	temperature of the cold side of the thermoelectric generator (°C)
T_h	temperature of the hot side the thermoelectric generator (°C)
T_{h-cond}	temperature of heat pipe condenser (°C)
T_{h-evap}	temperature of heat pipe evaporator (°C)
UA	rate of heat loss from the storage tank per unit temperature difference (W/°C)
R_w	thermal resistance for heat transfer from heat pipe to water (°C/W)
R_{hp}	thermal resistance offered by the individual heat pipe (°C/W)
N_{hp}	number of heat resistance (°C/W)
$R_{contact}$	contact thermal resistance (°C/W)
R_{TEG}	thermal resistance of each thermoelectric generator (°C/W)
N_{TEG}	number of thermoelectric generators

have got the leading share in global usage of solar water heating systems (Global status report, 2013) (see Fig. 1).

Broad categorization of solar water heating systems is presented by Raisul Islam et al. (2013) in his review paper. He categorizes solar water heating systems in 5 types as follows, thermosyphon systems (passive systems) Kalogirou, 1997; Gupta and Garg, 1968, integrated collector storage system (passive) (Smyth et al., 2006), direct circulation system (active) (Li et al., 2010), indirect water heating system (active) (Chaturvedi et al., 1998), and Air system (active) (Xu et al., 2006).

All the solar hot water systems presented by Raisul Islam et al. (2013) in his review paper are mature

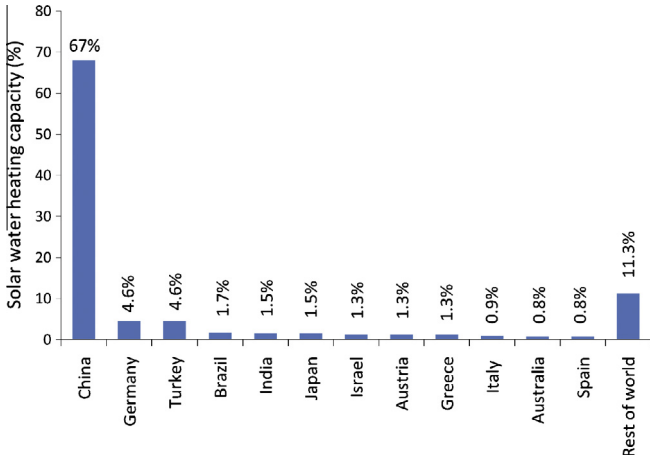

Fig. 1. Global share of the countries in 2011 for installed and operative solar water heating capacity (Global status report, 2013).

technologies and able to heat the water close to its boiling temperature at atmospheric pressure. There have been attempts made in the past to utilise this thermal energy from the solar heated water to solely generate electricity or combine it with power generation and hot water supply. Hu et al. (2010) has demonstrated the use of solar energy to assist power generation in conventional coal fired power generation plants. Whereas Quoilin et al. (2011) has presented a design to utilise solar thermal energy with an organic Rankine cycle solely for power generation. Few researchers have investigated using the hot water from the evacuated solar collector with thermoelectric generators and using an active water cooling system to generate power (Date et al., 2014). The hot water after circulating over the thermoelectric generator can be used for domestic hot water needs. This system has a limit on the hot side temperature of the thermoelectric generator since the water can be heated at maximum to 100 °C under atmospheric pressure in the evacuated tube solar collectors. Zheng et al. (2014) has proposed an active system with thermoelectric cogeneration for domestic purpose using the thermal energy from the water heating boiler and solar energy.

Significant amount of work research has been done on the photovoltaic thermal technology since 1970s (Chow, 2010) and low concentrated photovoltaic thermal technology during last decade (Yadav et al., 2013). Photovoltaic thermal system converts the small part of light energy directly to electrical energy while harvesting the large amount to thermal energy that can be easily stored and used for low grade energy applications such as space or

water heating for domestic or industrial purpose. Min and Rowe (2002) has proposed a system with symbiotic application of power generation and fluid heating in his design. Following this (Qiu and Hayden, 2009) proposed a system with thermoelectric power generation using the natural gas fired heat source and utilising the heat from cold side of TEG for water heating. Recently Zheng et al. (2013) has tried to incorporate thermoelectric power generation and combined water heating using the heat source as non-concentrated solar energy. This paper presents a combined water heating and power generation system using solar concentrator and thermoelectric generators. The proposed system is designed for the domestic solar water heating application that can also generate electricity using the thermoelectric generators. A typical solar water heating system transfers the heat using various active and passive methods and different working fluids to the water in the storage tank. The proposed system utilises this flow of heat to generate electricity using the thermoelectric generator and heat pipes as passive devices to transfer the heat to the water storage tank. A solar concentrator is used instead of evacuated collector in this system. Using a solar concentrator the system can achieve high heat flux desirable for better performance of the thermoelectric generators, and also achieve high temperature on the hot side of thermoelectric generators. Heat pipes are used to extract the heat from the cold side of the thermoelectric generator and the condenser of the heat pipes is immersed in the water storage tank. Another advantage of using heat pipes for heat transfer is their high heat flux carrying capacity that is useful when used to transfer heat from the solar concentrated target.

Table 1 describes the parameters of the heat pipes that are used in this research.

Using this approach there is an advantage for power generation because of the high heat flux and high temperature from the solar concentrator. Further sections illustrate the detailed mathematical modelling of the proposed system and experimental validation of the predicted results. Finally a case study of a standard house is presented with system design and sizing for its hot water demands.

2. Preliminary investigation and mathematical modelling

This section presents the detailed theoretical analysis of the proposed system for thermoelectric power generation using passive cooling and heat scavenging for domestic or industrial water heating. Incident solar radiation is concentrated using the Fresnel lens and directed towards the hot side of the thermoelectric generator. An aluminium heat spreader block is attached on the cold side of the thermoelectric generator. The evaporator of the heat pipe is embedded in the aluminium heat spreader. The condenser of the heat pipe is immersed in the water to dissipate the heat from the cold side to maintain the temperature difference between the hot and cold side of the thermoelectric generator. The water tank is insulated such that the heat dissipated from the thermoelectric generator cold side can be scavenged and stored in the form of hot water that can be used for domestic application.

Table 1
Heat pipe parameters.

Heat pipe parameter	Value
Outer diameter of heat pipe	6 mm
Wall thickness of heat pipe	0.2 mm
Length of heat pipe	200 mm
Material of pipe	Copper
Material of wick	Copper
Wick structure	Copper fibre wick

Incident solar radiation is concentrated using a Fresnel lens and directed towards the target heat spreader plate. The amount of heat reaching the target spreader plate depends upon the direct incident solar radiation perpendicular to the surface of the Fresnel lens, surface area of the lens and the transmission efficiency of the lens. Eq. (1) and Fig. 2 illustrate the heat reaching the target spreader plate.

$$\dot{q}_h = q''_{in} \times A_{lens} \times \eta_{lens} \tag{1}$$

The specific heat of water is 4200 J/kg K. We assume that the proposed system consists of a considerably larger mass of water in the reservoir than the mass of the thermoelectric generators and the target heat spreader at the back of the TEG. This way we can comfortably neglect the thermal mass of thermoelectric generator and aluminium heat spreader in our theoretical calculations.

Applying the conservation of energy principle and assuming that the thermoelectric generator, cold side spreader and the middle section of the heat pipe are well insulated and there are no heat losses from these sections we can write the energy balance as

$$\dot{q}_h = \dot{q}_w + \dot{q}_l + \dot{q}_{l-tar} + \dot{W}_{TEG} \tag{2}$$

Here $\dot{q}_h$ is heat reaching the hot side of thermoelectric generator, q_w is the sensible heat absorbed by the water in the tank, $\dot{q}_l$ is the heat lost from the water tank and $\dot{q}_{l-tar}$ is the heat lost from the target of a solar concentrator and $\dot{W}_{TEG}$ is power generated by the thermoelectric generator. This analysis is for the indoor lab based test setup as shown in Fig. 2, the heater and heat spreader will be insulated and this test setup uses single thermoelectric generator for testing. Hence for the following analysis it is assumed that the losses from the heater and the heat spreader are negligible and $\dot{q}_{l-tar}$ is not considered in the further equations. The power generated from thermoelectric generator is also ignored in the further analysis since the conversion efficiency from thermal energy to electrical energy of thermoelectric generator is 1–2%. For a real case scenario when the setup size is considerably large one must consider the convection and radiation losses from the target as well as the power generated from the thermoelectric generators in the energy balance equations.

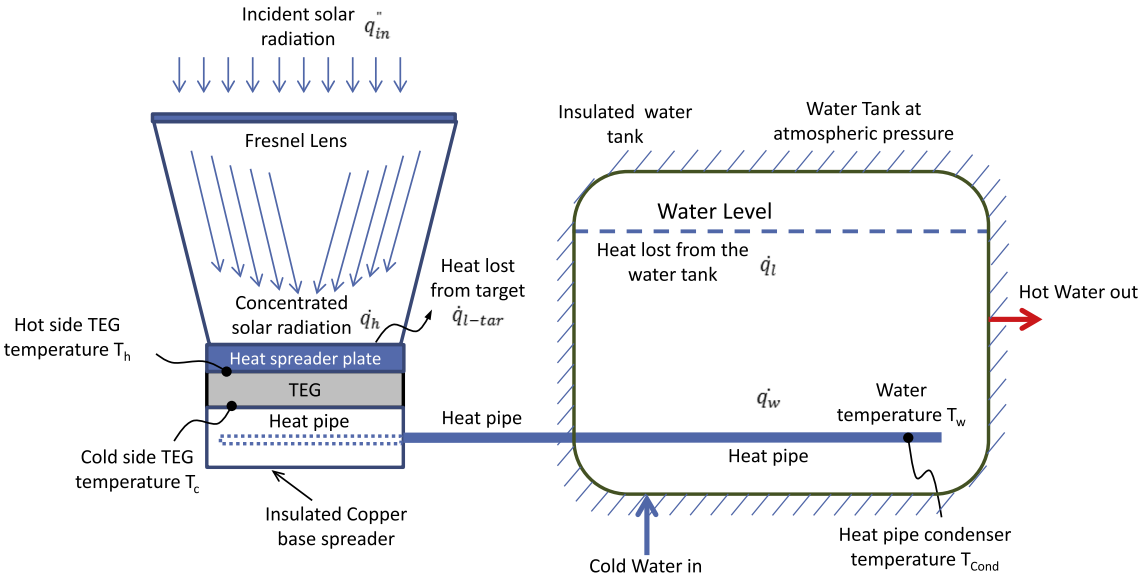

Fig. 2. Schematic of proposed system for thermoelectric power generation using passive cooling and heat scavenging for domestic or industrial water heating.

Sensible heat absorbed by the water can be expressed as

$$\dot{q}_w = m \times c_p \frac{dT_w}{dt} \tag{3}$$

Heat lost from the water tank can be expressed as

$$\dot{q}_l = UA_s(T_w - T_a) \tag{4}$$

Eq. (2) can be rewritten as

$$\dot{q}_h = m \times c_p \frac{dT_w}{dt} + UA_sT_w - UA_sT_a \tag{5}$$

The above equation is a first order, non-homogeneous, linear differential equation. Rearranging the above equation,

$$\dot{q}_h + UA_sT_a = m \times c_p \frac{dT_w}{dt} + UA_sT_w \tag{6}$$

Solution of the homogeneous part of the equation will be as follows,

$$UA_sT_w = \dot{q}_h + UA_sT_a \tag{7}$$

Particular solution of the non-homogeneous part of the equation will be as follows,

$$mC_p \frac{dT_w}{dt} = -UA_sT_w \tag{8}$$

Solving the above equation

$$\ln T_w = -\frac{UA_s}{m \times c_p} t \tag{9}$$

General solution of the non-homogeneous equation is given by the sum of the solution for homogeneous equation and the particular solution for the non-homogeneous equation.

Solving the above equation and combining the equations

$$T_w = C \cdot \exp\left[-\frac{UA_s}{m \times c_p} t\right] + \left[\frac{\dot{q}_h + UA_sT_a}{UA_s}\right] \tag{10}$$

Here "C" is the constant.

Now we can use the initial condition when time is zero. T_i is the initial temperature of the water when $t = 0$ the temperature of water T_w will be equal to T_i

$$T_i = C + \frac{\dot{q}_h + UA_sT_a}{UA_s} \tag{11}$$

Rearranging the above equation

$$C = T_i - \frac{\dot{q}_h + UA_sT_a}{UA_s} \tag{12}$$

Substituting the above equation to find the temperature of water

$$T_w = \left[T_i - \frac{\dot{q}_h + UA_sT_a}{UA_s}\right] \exp\left[-\frac{UA_s}{m \times c_p} t\right] + \left[\frac{\dot{q}_h + UA_sT_a}{UA_s}\right] \tag{13}$$

Using this solution of the first order non-homogeneous linear differential equation we can predict the transient behaviour of the temperature of water in the tank.

Once we predict the temperature of water in the tank we can predict the temperature of the various locations in the system such as the condenser and evaporator of the heat pipe, the cold side of the thermoelectric generator and the hot side of the thermoelectric generators. All the commercially available thermoelectric generators have a temperature limit for the hot side to avoid melting of the solders that are used to connect the thermoelectric material with the connector plates. Most commercially available generators have the limiting temperature within the range of 150–300 °C. Due to this structural stability factor it is

important to predict the hot side temperature of the thermoelectric generator.

Fig. 2 shows the schematic layout of the system where it is shown that a section of heat pipe is immersed in the water tank. If the water temperature is predicted to be below the local boiling temperature, the heat transfer regime between the outer surface of the immersed heat pipe section and the water in the tank will be similar to free convection over long horizontal cylinders. Solving the heat transfer correlations discussed by Churchill and Chu (1975) for the present system the outer surface temperature of the immersed section of heat pipe (heat pipe condenser) can be calculated.

If the water temperature is predicted to be equal to the local boiling temperature, the regime of heat transfer between the outer surface of the immersed heat pipe section and the water in the tank is assumed to follow typical boiling curve for water at 1 atmosphere (Incropera, 2002). Here the mode/regime of heat transfer will depend on the temperature difference between the outer surface of the heat pipe and local temperature of the water in the tank. For the known surface area of immersed section of the heat pipe, number of heat pipes and the rate of heat supplied, the available heat flux at the water tank can be calculated as,

$$\dot{q}''_{w_{hp}} = \frac{\dot{q}_h}{N_{hp} \times A_{hp-cond}} \tag{14}$$

Knowing the heat flux, the degree of super heat (excess temperature) between outer surface of immersed section of heat pipe and water in the tank can be estimated using typical boiling curve for water at 1 atmosphere. Now the surface temperature of the immersed section of heat pipe (heat pipe condenser) can be estimated using the water temperature calculated from Eq. (13) and the degree of super heat estimated from the typical boiling curve.

Fig. 3 illustrates the thermal resistance circuit for thermoelectric power generation system. Using the heat pipe condenser temperature estimated from the earlier step and the thermal resistance of the heat pipe as supplied by the manufacturer, the heat pipe evaporator temperature can be calculated as follows,

$$T_{hp-evap} = T_{hp-cond} + \dot{q}_h \times \left(\frac{R_{hp}}{N_{hp}}\right) \tag{15}$$

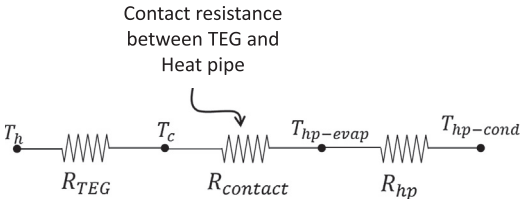

Fig. 3. Thermal resistance circuit for thermoelectric power generation system.

Since the hot water system is open to atmosphere, the temperature of water will never go above 100 °C. However for domestic applications, we will prefer to have the water temperature maintained at 80 °C.

The evaporator of the heat pipes are embedded in the aluminium heat spreader block and thermoelectric generator cold side is attached to the heat spreader block using the heat transfer gel. It is worth mentioning that the thermal contact resistance will depend upon the surface finish of the contact surfaces as well as the conductivity of the heat transfer gel and the thickness of the heat transfer gel layer which is proportional to the pressure applied to connect the contact surfaces. Overall contact resistance can be calculated knowing all the parameters mentioned above. Assuming that the thermal resistance offered by the aluminium heat spreader block is negligible, the temperature of the cold side of the TEG can be found as follows,

$$T_c = T_{hp-evap} + \dot{q}_h \cdot R_{contact} \tag{16}$$

Thermal resistance of each thermoelectric generator can be found from the manufacturer's catalogue. For this research the thermal resistance of the thermoelectric generator was measured experimentally and verified with the manufacturer's catalogue. Hot side temperature of the thermoelectric generator is predicted by knowing the thermal resistance of the thermal resistance of each TEG and number of TEG's being used in parallel.

$$T_h = T_c + \dot{q}_h \times \left(\frac{R_{TEG}}{N_{TEG}}\right) \tag{17}$$

From the above equations it is evident that the hot side temperature of the thermoelectric generator can be varied by changing the number of TEG's. That means the temperature of the hot side of TEG is a function of the heat flux flowing through it.

3. Validation of mathematical modelling

This section presents an experimental setup and testing method to validate the mathematical model presented in the earlier section for predicting the temperature of the water in the tank. In the proposed system, the heat source for thermoelectric power generation is suggested to be concentrated solar thermal devices such as Fresnel lens to achieve the high heat flux required by the thermoelectric generators. To validate the mathematical model an indoor testing setup was proposed to avoid the hurdles due to the inconsistent nature of weather in Melbourne, Australia. The concentrated solar thermal heat source was simulated on a small scale for lab testing and validation of the theoretical results using electric heaters (see Fig. 4).

Indoor experimental setup is designed to accommodate single thermoelectric generator (40 mm × 40 mm) sandwiched between the electric resistive heating plate and the cold side base spreader. Thermoelectric generator manufactured by Tellurex with 127 junctions and a maximum operating hot side temperature of 300 °C is used in this

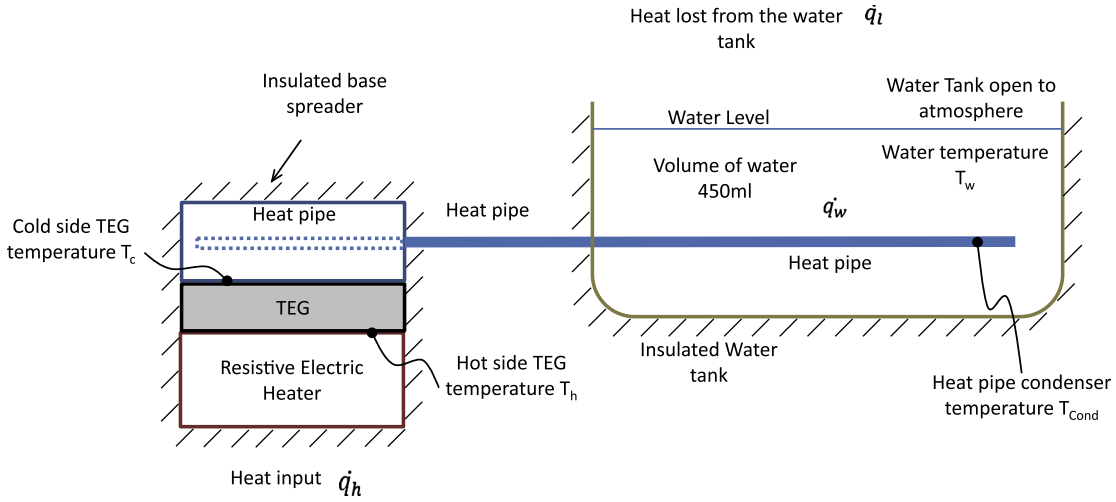

Fig. 4. Schematic of indoor testing setup for simulation of concentrated solar heat flux for thermoelectric power generation using passive cooling and heat scavenging for domestic or industrial water heating.

experiment. Four heat pipes each having 6 mm diameter and 200 mm length are used for heat transfer from the cold side of thermoelectric generator to the water tank for this experiment. Evaporator of the heat pipes is embedded inside the heat spreader block and the condenser is immersed inside the water in the tank. An acrylic water tank with 450 ml of volume is used in this experiment. Thermal paste was used to minimize the contact resistance between all the surfaces that are in physical contact and are meant to transfer the heat (see Fig. 5).

The above picture shows the heat pipes evaporator embedded in the aluminium heat spreader and the condenser inserted in the acrylic tank. The acrylic water tank has a volume of 450 ml. The heat pipes used in this experiment are 6 mm diameter and 200 mm long micro groove pipes. The wick of the heat pipe is made from 140 strands of copper fibres with each fibre being 8 μm in diameter. The numbers of heat pipes were chosen considering the diameter of the heat pipe, the size of the thermoelectric generator and the heat carrying capacity of each heat pipe. 40 mm of the heat pipe is embedded in the aluminium heat spreader while 20 mm is an adiabatic section, and rest 140 mm is the condenser inserted inside the acrylic water tank. The condenser length of the heat pipe to be immersed inside the water in the acrylic tank is 3.5 times the length of the evaporator (see Fig. 6).

The above figure illustrates the small scale lab based experimental setup for thermoelectric power generation with passive cooling and consequent water heating. A resistive electric heater is embedded in a block of aluminium to simulate the solar concentration from the Fresnel lens. A variable voltage transformer is used with a digital voltmeter and ammeter to measure the rate of energy input to the heater block. Digital voltmeter has a least count of 0.1 V and ammeter has a least count of 0.1 A. K type thermocouples were used to measure the temperature at various locations. Open circuit voltage from the thermoelectric generator was continuously measured. TEG was loaded and the maximum power output was measured for each steady state condition. An Agilent data logger was used to record the transient and steady state data. Table 2 illustrates the accuracies of all the instruments used for measurement during this research.

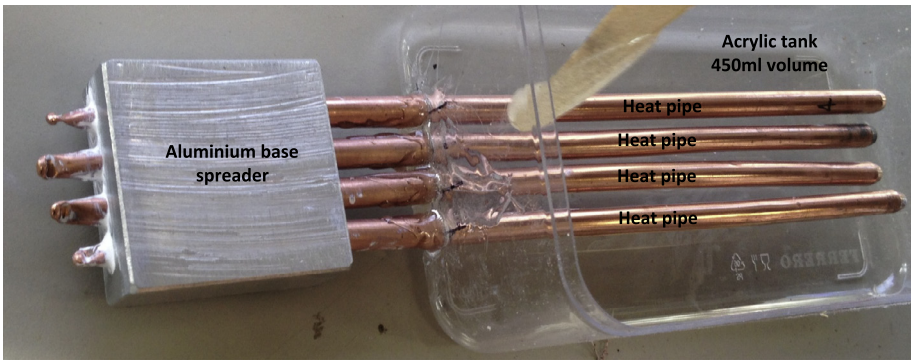

Fig. 5. Picture of heat pipe evaporator embedded in aluminium base spreader and condensor inserted in the acrylic water tank.

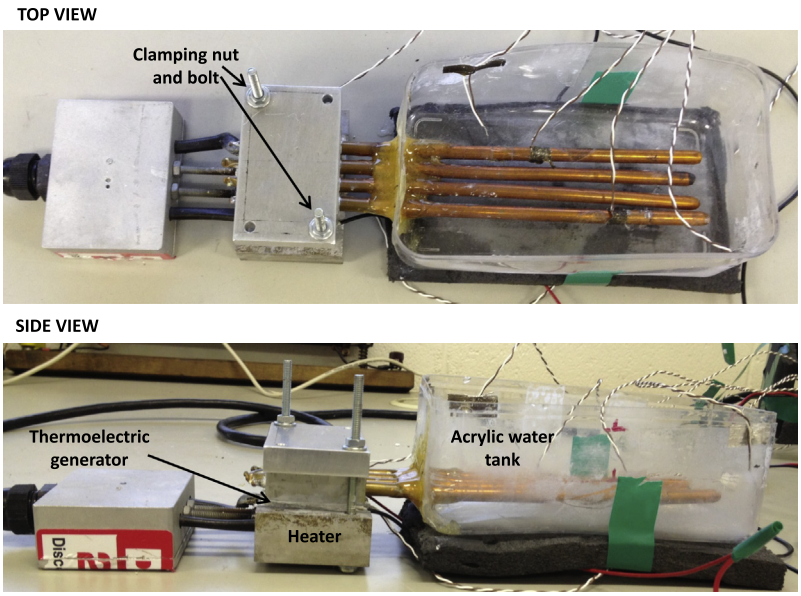

Fig. 6. Top view and side view of the whole experimental setup with electric heater, thermoelectric generator, heat pipe and water heating tank.

Table 2
Accuracies of instruments

Instrument	Parameter measured	Instrument precision
Digital multimeter (AC)	Voltage	±0.1% of reading
Digital multimeter (AC)	Current	±0.1% of reading
K-type thermocouple	Temperature	±0.5 °C
Agilent data logger (34972A)	DC voltage	±0.5% of reading
Agilent data logger (34972A)	DC current	±0.13% of reading

4. Determining the rate of heat loss from the insulated water tank

The Acrylic water tank used in the experiment is insulated using 15 mm thick black foam that covers the tank on all the sides. The water surface is insulated using the white polystyrene balls as shown in Fig. 7. These insulations simulate the conditions of the actual hot water storage tank used in conjunction with the conventional water heating systems. The variable UA_s (W/K) in Eq. (5) represents the rate of heat lost per unit temperature difference from the specific configuration of the water tank. Primary experiments were performed to estimate the for the water tank used in this experiment.

Temperature decay profile with respect to time was recorded for the water tank to estimate the UA_s for the water tank in use. Water temperature decay is recorded for two configurations, one with insulation on the water surface and one without insulation on the water surface. Water in the tank was heated to a certain temperature and the heat input then switched off and the water let to cool down to the ambient temperature. Eq. (5) in the earlier section shows the energy balance with heat input $\dot{q}_h$ heat absorbed by water $\dot{q}_w$ and the heat lost from the water tank $\dot{q}_l$. Since the heat input is switched off to record the temperature decay, Eq. (5) can be re written as

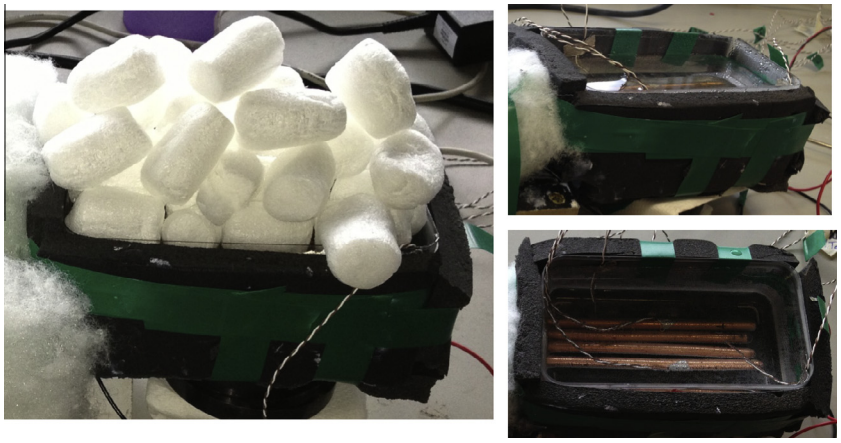

Fig. 7. Insulated water tank.

$$-m \times c_p \frac{dT_w}{dt} = UA_s(T_w - T_a) \quad (18)$$

Here $\frac{dT_w}{dt}$ is the slope of the decay of water temperature with time, and is the mass and specific heat of water. $(T_w - T_a)$ is the difference between the water temperature and ambient temperature (see Fig. 8).

Using the Eq. (21) and $\frac{dT_w}{dt}$ from the above graph, we can estimate the rate of heat loss from the water tank per unit temperature difference. The heat input of 60 W was supplied to the TEG and the system was allowed to reach the steady state condition. Once the steady state condition was reached, the heat supply was cut off and the water was allowed to cool down to the ambient temperature, while measuring the water temperature decay of with respect to time. The average value of UA_s for the water tank after 60 W of heating had been applied is 0.88 W/K determined using Eq. (21) for the temperature decay over time (see Table 3).

5. Results and discussion

The thermoelectric generator with the specifications mentioned in Table 4 was used for the investigation in this research. Various heat fluxes were applied across the thermoelectric generator while maintaining the hot side temperature of the TEG at or below 300 °C.

The cold side temperature of the thermoelectric generator is dictated by the amount of heat flux supplied and the number of heat pipes used to transfer the heat to the water tank. Water temperature cannot go above 100 °C since the water tank was maintained at atmospheric pressure.

The amount of heat supplied to the setup was varied from 20 W to 80 W with steps of 20 W. The following figure shows the predicted water temperature for all the 5 heat input conditions (see Fig. 9).

In the above graph it is observed that the predicted thermal equilibrium temperature of water is 35 °C when the heat input is 20 W, 55 °C when the heat input is 40 W, 75 °C when the heat input is 60 W and 95 °C when the heat input is 80 W with fixed rate of water cooling from the tank.

Table 3
Values of UAs with respect to temperature of water T_W.

Water temperature T_W (°C)	UA_S (W/°C)
35	0.76
40	0.80
50	0.86
60	0.91
70	0.96
74	0.99

Table 4
Properties of the thermoelectric generator under study.

Properties	Value (unit)
Number of thermoelectric couples	127
Length (l) × width (w) × height (h)	40 × 40 × 3 (mm)
Hot side maximum temperature (T_h)	300 °C
Maximum power output @$\Delta T = 200$ °C	5.7 W
Maximum current (I_{SC})	1.3 A
Maximum open circuit voltage (V_{OC})	4.2 V
Thermal resistance (R_{TEG})	1.5 °C/W
Ceramic material	Alumina (Al_2O_3)

However in actual setup the value of UA_s will vary with the rate of heat input and the water temperature. The value of is measured for various heat inputs and water temperatures for the theoretical prediction of the temperature of water. Fig. 10 illustrates the comparison between the transient behaviour of the predicted and experimental water temperature. Estimated steady state temperature for a heat input rate of 20 W is 53 °C while the experimental steady state water temperature is 49 °C. Similarly for heat input rate of 40 W, 60 W and 80 W the predicted steady state temperatures were 68 °C, 75 °C and 83 °C respectively while the measured steady state temperature were 65 °C, 71 °C and 79 °C respectively.

All the graphs show reasonable agreement between the theoretical predictions and experimental results of transient temperature rise as well as steady state water temperature.

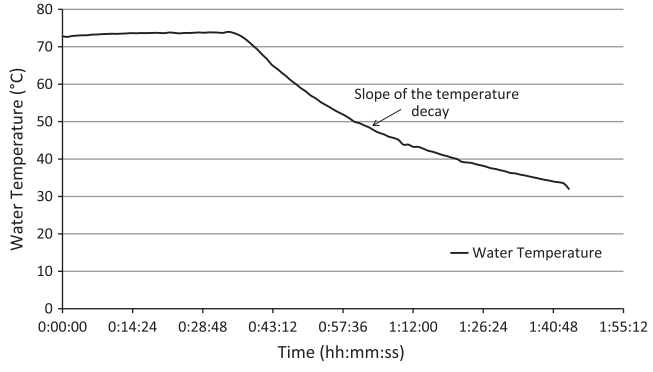

Fig. 8. Water temperature decay without insulation on the surface of the water.

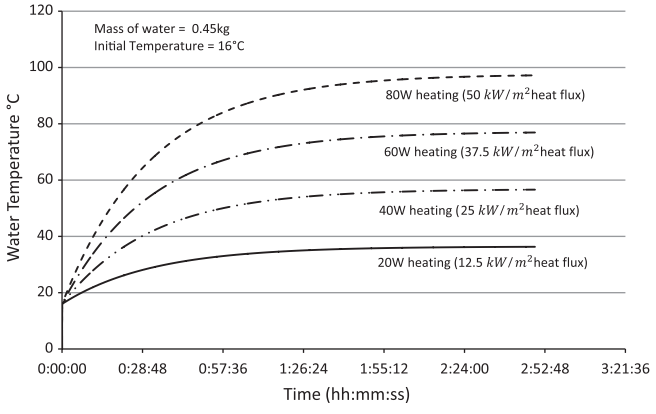

Fig. 9. Transient behaviour of water temperature under various heat inputs and fixed "UA_s" for cooling of water reservoir.

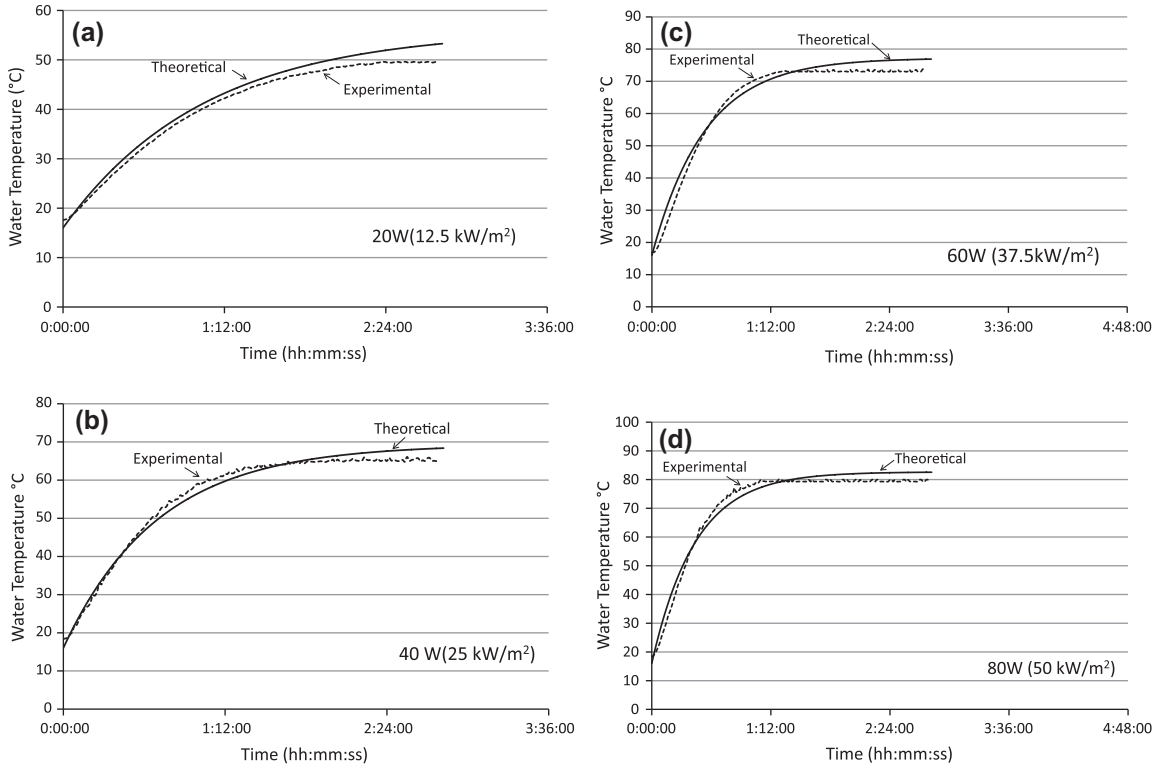

Fig. 10. Comparison between predicted and experimental results for water temperature at different power inputs (a) 20 W (12.5 kW/m^2), (b) 40 W (25 kW/m^2), (c) 60 W (37.5 kW/m^2), and (d) 80 W (50 kW/m^2).

The small difference between the experimental and theoretical results can be accounted for following reasons:

- Uncertainty in the experimental measurements due to instrumental accuracy.
- Power extracted from the TEG is neglected in the theoretical analysis.
- Theoretical analysis neglects heat loss due to surface evaporation in the water tank.

By knowing the rate of heat loss from the water storage tank we can predict the transient and steady state behaviour of the water temperature very closely.

Fig. 11 presents the experimental results for the test setup with 60 W heat input to the single thermoelectric generator with 4 heat pipes to transfer the heat from the cold side of the TEG to the water tank containing 450 g of water. The graph presents experimental results for transient behaviour of TEG hot side temperature, TEG cold side temperature, TEG open circuit voltage and water temperature. The temperature difference between the hot and cold side of the thermoelectric generator is calculated and presented on the same graph for comparison. For 60 W heat input maximum hot side temperature at steady state reaches 154 °C while the cold side steady state temperature reaches 94 °C. It takes approximately 65 min for the TEG hot side, TEG cold side and water temperature to reach steady state. Although it can be clearly seen that the temperature difference between the hot side and the cold side of the TEG achieves its steady state of 54 °C in approximately 12 min. Open circuit voltage of the thermoelectric generator is a direct function of temperature difference and therefore we can that it behaves in accordance with the temperature difference.

The thermal mass ($m \times c_p$) of the thermoelectric cell, the aluminium heat spreader and the heat pipes together is significantly smaller (1/28th) than the thermal mass of the water in the system. Due to this reason the temperature difference between the hot side and the cold side of the thermoelectric generator reaches steady state more quickly than the steady state of the hot and cold side temperatures itself. We can assume the whole system to be in the steady state at any time after the temperature difference reaches its steady state due to the negligible thermal mass of the system components compared to the thermal mass of water.

Fig. 12 shows the power generated by thermoelectric generator for ΔT of 60 °C and 150 °C. Maximum power generated by the thermoelectric generator in the lab setup for 60 W heat input and ΔT of 60 °C is 1.27 W, whereas that for the heat input of 180 W and ΔT of 150 °C is 3.5 W. Thermoelectric power generation efficiency can be calculated using the following equation

$$\eta_{TEG} = \frac{\dot{W}_{TEG}}{\dot{q}_h} \times 100 \tag{19}$$

Thermoelectric generator efficiency is 2.1% for 60 W heat input and ΔT of 60 °C across hot and cold side whereas 1.94% for 180 W heat input and ΔT of 150 °C.

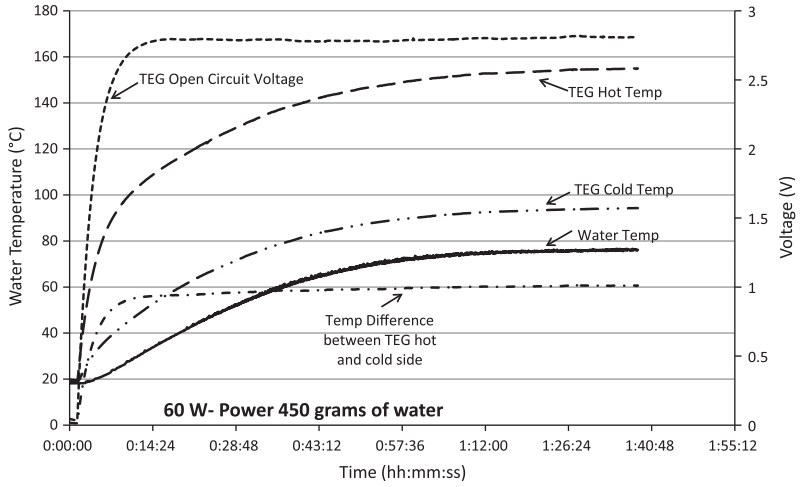

Fig. 11. Experimental results for 60 W heat input and 450 ml of water in the tank.

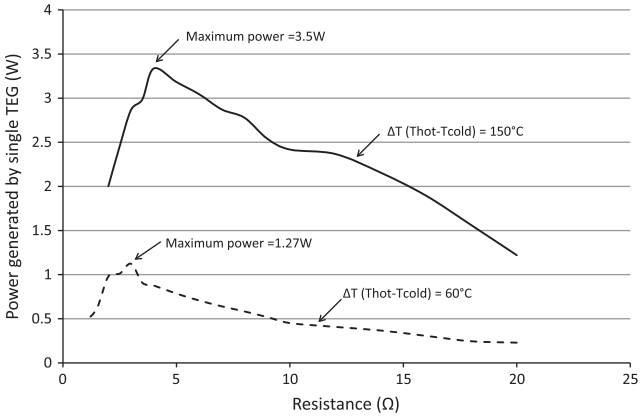

Fig. 12. Comparison of thermoelectric power for two different temperature differences between the hot and cold sides.

Conversion efficiency of the thermometric generator used for these experiments is consistent with the manufacturer's specifications.

Whereas solar water heating efficiency can be calculated using the following equation

$$\eta_{\text{water-heating}} = \frac{\dot{q}_w}{\dot{q}_h} \times 100 \tag{20}$$

Heat absorbed by the water in the tank can be calculated by knowing the mass of water in the tank and the rate of bulk temperature rise of the water with respect to time. Heat absorbed can be also calculated by subtracting the target losses, tank losses and TEG power generation from the total heat input. Water heating efficiency of 53.8% is observed for heat input of 60 W and water temperature of 73 °C, whereas the water heating efficiency of 61.30% is observed for 180 W of heat input with water temperature 98 °C.

6. Case study

This section presents a case study and brief system sizing of the proposed design for the standard house in Melbourne for its domestic hot water needs and part of its electric demand. The case study will include considering the daily house hold hot water demand as well as electricity demand and propose a design and size the system to satisfy these demands using the solar concentrator system with thermoelectric generators and heat pipes for effective heat transfer between the cold side of thermoelectric generator and the water tank.

Parameters of a typical house in Melbourne that are being used for the case study are listed in Table 5.

As mentioned in the above table the surface area available for solar collector is 5 m^2. As mentioned in the earlier section the Fresnel lens solar concentrator is proposed to be used in this system. Assuming the optical efficiency of the Fresnel lens is 80% we can say that the total solar energy reaching the target of the solar concentrator is 3600 W.

Considering the F-number of Fresnel lens in the range of 0.8–1.2, the focal length of a single 5 m^2 lens will be in the range of 1.8–2.7 m. This will require the system to have large tall structure and make it bulky for a domestic application. To deal with this issue it is suggested to use multiple Fresnel lenses with cumulative collector aperture area of 5 m^2 to make the structural design simple and flat.

Typically a hot water storage tank will be cylindrical in shape with certain diameter and length or height. To calculate the surface area of the cylindrical tank with certain

Table 5
Various parameters for the typical house in Melbourne used for the system design and sizing.

Properties	Value (unit)
Total daily hot water consumption	400 l
Initial temperature of water	16 °C
Set temperature of water in tank	80 °C
Total daily electricity usage	7 kW h
Available roof surface area for solar collector	5 m^2
Direct incident solar radiation flux	900 W/m^2

volume of water in the tank we will assume that the length is always 1.5 times the diameter of the tank.

$$L = 1.5D \tag{21}$$

Volume of the cylinder is

$$V = \frac{\pi}{4}D^2L \tag{22}$$

Combining above equations we can express the diameter in terms of volume of the water needed to be stored in tank.

$$D = \sqrt[3]{0.8488 \cdot V} \tag{23}$$

In Eq. (15) the unknown parameter UA_s was determined experimentally. However this term can also be written as

$$\frac{A_s}{\frac{1}{U}} \tag{24}$$

The R-value of the insulating materials is a measure of thermal resistance to the flow of heat through the material. R-value is defined as ratio of temperature difference over heat flux $\left(\frac{\Delta T}{\dot{q}''}\right)$. Unit of R-value is $\left(\frac{m^2 \cdot K}{W}\right)$. This particular R-value considers the combination of all the relevant forms of possible heat transfer such as conduction, convection and radiation. Since UA_s was the measure of the rate of heat loss from the hot water storage tank in form of conduction convection and radiation and the R-value of any insulating material can be used in place of $\left(\frac{1}{U}\right)$ and we can write the above equation as follows.

$$\frac{A_s}{R_{\text{value}}} \tag{25}$$

Surface area of the tank exposed to the ambient that will account for the heat loss from the tank is A_s. Surface area of the cylinder is expressed as follows

$$A_s = \pi DL + 2\left(\frac{\pi}{4}D^2\right) \tag{26}$$

Substituting the value for D derived from the volume of the cylinder equation in the above equation

$$A_s = \pi\left(\sqrt[3]{0.8488 \cdot V} + 0.5(\sqrt[3]{0.8488 \cdot V})^2\right) \tag{27}$$

Combining Eqs. (15), (26), and (28) we can find the temperature of water in terms of the volume of water to be heated and R-value of the insulating material being used for the hot water storage tank. We assume the hot water storage tank uses the 30 mm thick layer of glass wool insulation of the tank with R-value of 0.75 W/K in SI units. The transient behaviour of the water temperature in the storage tank of 400 l capacity can be determined using the mathematical model presented in the earlier section. Maximum water temperature in the tank is set to be 80 °C for domestic purpose. We can predict the time required to heat up the required mass of water from ambient temperature to the maximum set temperature with the available heat input from the sun. This will be the time that we will need to track the sun and once the set temperature is reached in the tank, the tracking will be switched off. When there is no heat input from the sun, the heat will be lost from the hot water storage tank and this rate of heat loss can be predicted using the same mathematical model.

Here R-value per unit mass of water in the storage tank is comparatively lot smaller than that in the test setup discussed in the earlier section.

R-value per unit mass for the case of this example is $\frac{0.75\frac{W}{K}}{400\ kg}$, which is equal to 0.001875 W/K kg, whereas the similar ratio for the lab test setup is $\frac{0.88\frac{W}{K}}{0.45\ kg}$, which is equal to 1.95 W/K kg. Due to very small value of R per unit mass the temperature rise during heat input as shown in Fig. 13 appears to be close to linear and does not show the sharp curvature like seen in curves for water heating in Figs. 10 and 11.

For this case study it is considered that we use the Fresnel lens with optical efficiency of 80% and surface area of 5 m^2 tracks the sun in single axis during the peak sun hours with direct incident solar radiation of 900 W/m^2. From above figure we can see that 300 l of water stored in the insulated tank can be heated from 16 °C to 76 °C during the peak sun hours. While the time when the energy from the sun is not available, the heat is lost from the insulated tank and the temperature of water will drop top 67 °C during remaining 18 h of the day.

7. Sizing of the thermoelectric generator and heat pipes

It is proposed in the system to utilise the flow of heat from the solar collector to water to generate electricity using the thermoelectric generators. Dimensions and the physical properties of the thermoelectric generator are as mentioned in Table 1. Thermal resistance of each thermoelectric generator is 1.5 °C/W with maximum allowable hot side temperature of 300 °C. All the thermoelectric generators will be connected in parallel with each other. Overall thermal resistance offered by the thermoelectric generators will be equal to $\frac{R_{TEG}}{N_{TEG}}$.

$$\dot{q}_h = \frac{(T_h - T_c)}{\frac{R_{TEG}}{N_{TEG}}} \tag{28}$$

For the heat input of 3600 W and to maintain the temperature difference of 60 °C we will need to have 90 thermoelectric generators at the target of the solar concentrator. These 90 TEG's can generate 114 W for 6 h. That will be equivalent to 0.685 kW h. Whereas for the heat input of 3600 W and to maintain temperature difference of 150 °C we will need to have 36 thermoelectric generators at the target area and these TEG's can generate 126 W for 6 h or in other words it can generate 0.756 kW h energy from the flowing heat. From the above analysis we can observe that having lower number of TEG's and maintaining larger temperature difference can generate larger amount of electricity. This of course

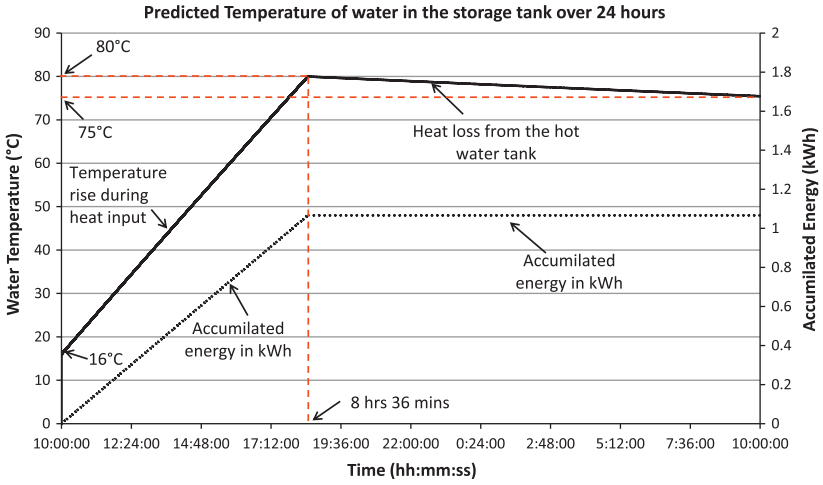

Fig. 13. Predicted transient behaviour of temperature of water in the tank during 24 h cycle.

requires that the Fresnel lens and target achieve a greater concentration of the solar energy to give 3600 W on the smaller area.

Each thermoelectric generator is 40 mm long and 40 mm wide in its dimensions and the target area will be 0.0576 m^2 for 36 TEG's those can generate 0.756 kW h. With the aperture area of 5 m^2 we will need to have a geometric solar concentration of approximately 86 suns to focus the entire solar radiation incident on aperture of the lens to the target area.

Heat pipes of 6 mm diameter are proposed to be used for transporting the heat from the cold side of the thermoelectric generator to the hot water storage tank. Using the information from the experimental setup, we can assume that under the cold side of each TEG with 40 mm × 40 mm we can attach 4 heat pipes with diameter 6 mm. Depending upon the type of solar concentrator device there can be various configurations in which the TEG's can be fitted at the target area. In this case study we will consider one of the possible configurations for the TEG's to be fitted at the target area using the square Fresnel lens at the aperture and a square target. A square target will have 6 TEG's along its length and 6 TEG's along width of the target. With 6 TEG's along the length we can accommodate 24 heat pipes in line. The overall thermal resistance offered by the heat pipes connected in parallel thermal circuit will be 0.008333 °C/W and the temperature difference between the evaporator and the condenser of the heat pipes will be approximately 30 °C.

A combined solar water heating and power generation system that can meet the daily hot water demand (400 l) of a typical house with 4 occupants and supply an added 0.756 kW h of electricity has thus been proportionated.

8. Conclusion

A novel system is proposed that can generate electricity and hot water utilising the flow of heat from a solar collector via a thermoelectric generator to hot water storage tank. The system also uses the solar concentrator improve the performance of thermoelectric generators and heat pipes to cool one side of TEG and passively transfer the heat to the water storage tank. Mathematical modelling is presented to predict the transient and steady state behaviour of the various temperatures in the proposed system. Lab experiments have been performed to validate the mathematical model predictions. An important part of this modelling is the knowledge of value for the rate of heat loss from the hot water storage tank. A case study with a system design of basic components is presented for a typical house with 4 occupants and daily hot water demand of 400 l. It is determined that having less TEG's, a higher concentration ratio and hence higher temperature difference will produce more electric power than having more TEG's and less temperature difference. For a typical house with 5 m^2 of available surface area 300 l of water can be heated to 76 °C during the peak sun hours such that minimum solar tracking is required and thermoelectric generators can generate 0.756 kW h of electricity at the same time. According to the predicted results the 300 l of water stored in the insulted tank will lose around 9 °C temperature dropping from 76 °C to 67 °C, over the period of 18 h when the heat is not supplied to the tank.

References

Best, F.G., Riffat, S.B., 1995. Miniature combined heat and power system. Renew. Energy 6 (1), 49–51.
Butti, K., Perlin, J., 1979. Early Solar Water Heaters – A Golden Thread. Van Nostrand Reinhold Company, New York.
Butti, K., Perlin, J., 1981. A Golden Thread – 2500 years of solar architecture and technology. Marion Boyars Publishers Ltd., London.
Chaturvedi, S.K., Chen, D.T., Kheireddine, A., 1998. Thermal performance of a variable capacity direct expansion solar-assisted heat pump. Energy Convers. Manage. 39 (3–4), 181–191.
Chow, T.T., 2010. A review on photovoltaic/thermal hybrid solar technology. Appl. Energy 87 (2), 365–379.
Churchill, S.W., Chu, H.H.S., 1975. Correlating equations for laminar and turbulent free convection from a horizontal cylinder. Int. J. Heat Mass Transfer 18 (9), 1049–1053.

Date, A., Date, A., Dixon, C., Akbarzadeh, A., 2014. Progress of thermoelectric power generation systems: Prospect for small to medium scale power generation. Renewable and Sustainable Energy Reviews 33, 371–381.

Gupta, C.L., Garg, H.P., 1968. System design in solar water heaters with natural circulation. Solar Energy 12 (2), 163–182.

Hu, E., Yang, Y., Nishimura, A., Yilmaz, F., Kouzani, A., 2010. Solar thermal aided power generation. Appl. Energy 87 (9), 2881–2885.

Incropera, F.P., 2002. In: DeWitt, D.P. (Ed.), Fundamentals of heat and mass transfer, 5th ed. Wiley, New York.

Kalogirou, S., 1997. Solar water heating in Cyprus: current status of technology and problems. Renew. Energy 10 (1), 107–112.

Kalogirou, S., 2009. Solar Energy Engineering: Processes and Systems. Elsevier, London.

Li, Z., Chen, C., Luo, H., Zhang, Y., Xue, Y., 2010. All-glass vacuum tube collector heat transfer model used in forced-circulation solar water heating system. Solar Energy 84 (8), 1413–1421.

Min, G., Rowe, D.M., 2002. "Symbiotic" application of thermoelectric conversion for fluid preheating/power generation. Energy Convers. Manage. 43 (2), 221–228.

Qiu, K., Hayden, A.C.S., 2009. A natural-gas-fired thermoelectric power generation system. J. Electron. Mater. 38 (7), 1315–1319.

Quoilin, S., Orosz, M., Hemond, H., Lemort, V., 2011. Performance and design optimization of a low-cost solar organic Rankine cycle for remote power generation. Solar Energy 85 (5), 955–966.

Raisul Islam, M., Sumathy, K., Ullah Khan, S., 2013. Solar water heating systems and their market trends. Renew. Sust. Energy Rev. 17 (0), 1–25.

Renewables 2013: Global status report, 2013, Renewable energy policy network for 21st century.

Smyth, M., Eames, P.C., Norton, B., 2006. Integrated collector storage solar water heaters. Renew. Sust. Energy Rev. 10 (6), 503–538.

Xu, G., Zhang, X., Deng, S., 2006. A simulation study on the operating performance of a solar–air source heat pump water heater. Appl. Therm. Eng. 26 (11–12), 1257–1265.

Yadav, P., Tripathi, B., Rathod, S., Kumar, M., 2013. Real-time analysis of low-concentration photovoltaic systems: a review towards development of sustainable energy technology. Renew. Sust. Energy Rev. 28, 812–823.

Zheng, X.F., Yan, Y.Y., Simpson, K., 2013. A potential candidate for the sustainable and reliable domestic energy generation – thermoelectric cogeneration system. Appl. Therm. Eng. 53 (2), 305–311.

Zheng, X.F., Liu, C.X., Boukhanouf, R., Yan, Y.Y., Li, W.Z., 2014. Experimental study of a domestic thermoelectric cogeneration system. Appl. Therm. Eng. 62 (1), 69–79.